DOI: https://doi.org/10.68732/6f01747ba5babf94

ISBN: 978-9989-2053-6-1

Development and application of experimental systems for the measurement of thermal properties in rocks using representative-size specimens

M. Herbón-Penabad, Y. Li, A. Muñoz-Ibáñez, J. Delgado-Martín& R. Juncosa-Rivera
Rock Mechanics Laboratory. Universidade da Coruña, Coruña, Spain
jorge.delgado@udc.es
0000-0002-4818-3964

A. Perez-Carreras, E. Ibañez-Martinez, J. M. Segura-Serra, J. Canal-Vila & J. Alvarellos-Iglesias
Repsol Technology Lab, Móstoles, Spain

Abstract

Understanding the thermal behaviour of rocks is essential for the safe and efficient design of geotechnical and energy engineering systems. Applications such as geological storage of CO_2, H_2, CH_4, LN_2 or air, underground heat storage, and the stability assessment of structures subjected to thermal gradients all depend on accurate knowledge of rock thermal properties. Thermal conductivity (λ), specific heat capacity (C_P), and the coefficient of thermal linear expansion (CTLE) must therefore be determined reliably. However, traditional methods often use milligram-scale or miniature samples, which may not adequately represent medium- to coarse-grained lithologies or capture key features such as porosity. This study introduces three experimental devices designed for core-plug size specimens, enabling the characterization of thermal properties in a wide range of conditions of igneous, metamorphic, and sedimentary rocks. The performance of each device was verified against reference materials with well-known thermal behaviour: Thermal conductivity is measured with an enhanced transient heat-flow, divided-bar system that can operate above and below ambient temperature with a maximum thermal gradient of ~520 °C; C_P is determined by drop calorimetry using glycerol as the calorimetric fluid; and CTLE is measured with a high-resolution (~1 µm) push-rod dilatometer. The calorimeter and the dilatometer can operate up to ~800 °C. The results highlight significant impacts derived from mineralogy, density, porosity, and anisotropy on rock thermal properties while confirm the adequacy and reliability of the experimental systems.

Keywords

Thermal properties, Thermal conductivity, Specific heat capacity, Coefficient of thermal linear expansion, Dilatometry, Temperature dependence.

1 Introduction

The thermal behaviour of rocks plays a fundamental role in a wide range of geological, geotechnical and energy engineering applications. Processes such as geothermal energy production, underground thermal energy storage, geological storage of fluids (e.g., CO_2, H_2, CH_4 or compressed air), nuclear waste disposal, or the assessment of the stability of underground structures subjected to thermal gradients strongly depend on the thermophysical properties of the host rock. In these contexts, heat transfer, heat storage capacity and thermally induced deformation can significantly influence both the efficiency and long-term safety of engineered subsurface systems. An accurate knowledge of these parameters is essential for reliable thermo-hydro-mechanical (THM) modelling of geological systems as well as for the safe design of engineering solutions involving thermal loadings.

In the assessment of thermal behavior of rocks, the ISRM Suggested Method (SM) identifies thermal conductivity (λ), thermal diffusivity (a), thermal effusivity (μ) and volumetric heat capacity (C) as key properties although it acknowledges that it is not necessary the measurement of all of them since they are mutually related(Popov *et al*., 2016). Thus, a and μ are defined by the relationship between λ and C according to the following expressions: $a=\lambda/C$ and $\mu=(\lambda \cdot C)^{1/2}$. Likewise, specific heat capacity, C_p is also related with C through rock density, ρ ($C_p=C/\rho$). However, ISRM does not include thermal expansion among the assessed thermal properties and thermal conductivity is only determined in a narrow temperature range close to ambient conditions. Furthermore, based on that work, here we extend the scope of the SM by considering the measurement of thermal conductivity (λ); specific heat capacity (C_p) and the coefficient of linear thermal expansion (CTLE or α) of rocks.

The thermophysical properties of rocks are strongly influenced by different factors such as mineral composition, grain size, density, porosity and other microstructural features such as bedding, foliation or microcracking. For instance, quartz-rich rocks tend to exhibit relatively high λ, whereas increasing porosity generally reduces heat transfer due to the lower λ of pore fluids or air (Zhu et al., 2022). Likewise, many rocks exhibit anisotropic thermal behaviour associated with preferred mineral orientations or stratified structures (Labus and Labus, 2018).

Despite their objective relevance, the experimental determination of rock thermal properties presents several challenges. Rocks are inherently heterogeneous materials, and their thermophysical behaviour may significantly vary even within a single lithology. Conventional laboratory techniques used to determine thermophysical properties, such as differential scanning calorimetry or laser flash analysis, usually require milligram-scale samples or thin specimens. Although these techniques offer high analytical precision, the small size of the tested samples may not adequately capture the heterogeneity of medium- to coarse-grained rocks or the influence of structural features that are relevant at larger scales. Thus, there is a compelling necessity to develop experimental approaches allowing the assessment of thermal properties of rocks using specimens of representative dimensions, such as those typically employed in rock mechanics testing.

In this context, the present work expands the scope of the currently available ISRM SM by describing the development and application of three experimental systems designed to determine these key thermal properties in rocks using plug-size specimens: An enhanced divided-bar apparatus for the determination of λ, a drop calorimeter for the measurement of C_p, and a high-precision, push-rod dilatometer for determiningα. These devices were designed to operate over a wide temperature range and to allow testing of a variety of lithologies representative of common geological materials.

2 Methodology

2.1 Heat capacity

Specific heat capacity, C_p, provides an estimation of the amount of thermal energy that can be stored within a given rock. It can be determined using the drop calorimetry method described in the ASTMD4611 standard. According to it, a rock specimen is heated to a known temperature, dropped into a calorimetric fluid of known thermal properties, and the equilibrium temperature of the mixture observed. Provided that there are not heat leaks, the heat released by the rock during cooling is equal to the heat absorbed by the calorimetric system.

The experimental setup (Fig. 1) is based on two main elements: A high-temperature, vertical tube furnace (which provides the heat source) and a cryogenic Dewar flask (which acts as calorimeter).

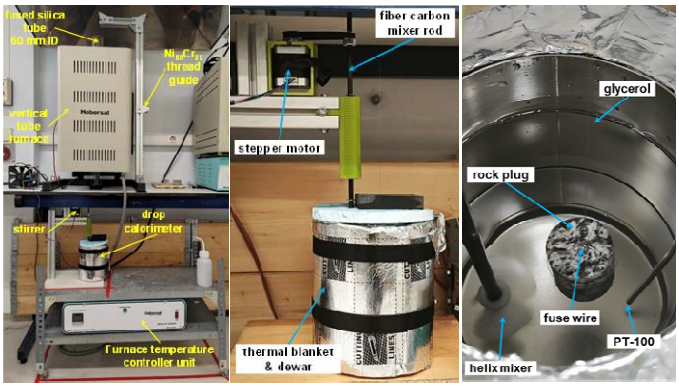


Fig. 1 Tube furnace on top of the calorimeter (left), Dewar flask with a stirring mechanism (center) and rock sample in the calorimetric fluid (right) used to assess constant pressure heat capacity C_P.

The tube furnace (*Hobersal* mod. HTF 116040) is able to operate at a maximum temperature of 1100 °C with a nominal power of 4 kW. According to the manufacturer's specifications, the furnace provides a 100 mm homogeneous heating zone centered along the geometric midpoint of a 400 mm total heated length. The furnace incorporates a fused silica tube (70 mm-OD, 60 mm-ID) where the rock specimen is introduced suspended from a thin nichrome wire (*Parr Inst.* 45C10) to prevent contact with the tube walls and ensure uniform thermal exposure during the heating phase. The calorimeter is based on a *KGW* GSS 1000W Dewar flask, which is a double-walled stainless-steel, thermally-isolated vessel with a nominal capacity of 1000 mL, 100 mm-ID and height of 156 mm that is filled with the calorimetric fluid. To prevent thermal stratification during the experiments in the fluid, the Dewar has been equipped with a simple mechanical stirring system (*i.e.*a stepper motor connected with a belt to a carbon-fiber rod fitted with a polymer propeller at its lower end). This mechanism ensures homogeneous thermal conditions throughout the duration of the thermal transfer. The Dewar flask is further thermally isolated with a thermal blanket and a *Styrofoam*™ lid through which it penetrates the axis of the stirrer as well as a high-precision PT-100 thermal probe connected to a high-resolution (0.001 ºC), high-accuracy (0.015 ºC) data acquisition module (*Pico Technologies* mod. PT-104).

Drop calorimetry provides with the constant-pressure heat capacity of the rock ($C_{P,r}$) and this can be obtained from an energy balance relationship:

$$C_{P,r} = \frac{((m_{fluid} - m_{evap})C_{P,fluid} + mc_p)\,(T_m - T_c)}{m_r(T_d - T_m)} \quad (1)$$

where m_r, m_{fluid}, m_{evap} are the mass of the test specimen, the mass of the calorimetric fluid and the mass of fluid evaporated when the immersion takes place, $C_{p,fluid}$ is the thermal capacity of the fluid, $T_d T_m$,T_c are temperature of the specimen when released from the furnace, the temperature of the mixture and the initial temperature of the fluid and mc_p is the thermal capacity of the system The calorimetric fluid used in the experiments is glycerol ($C_3H_8O_3$), and that was selected due to its low vapour pressure, high boiling point, and well-characterized thermophysical properties (Righetti et al., 1998). The calorimetric system was calibrated using a 99.9%-purity C101 (CW004A) copper sample, and its performance verified using a 99% α-Al_2O_3 ceramic specimen, both with known heat capacity values.

2.2 Thermal expansion

Thermal expansion refers to the increase in volume or length experienced by a rock due to the increase in temperature. In the case of linear expansion, α (or CTLE in engineering practice), this corresponds to the change on length per unit length per degree of temperature (K^{-1}). It determines the magnitude of thermally induced strains which may generate stresses with the potential of modifying the mechanical stability, permeability or fracture behaviour of a rock mass (Schön, 2015). To determine this property in rocks we have developed a simple push-rod dilatometer based on the considerations given in the ASTM E228 standard. In this system, a properly shaped rock plug (ISRM, 1979) is placed inside a

heated chamber where its length variation is transmitted through a fused-silica push-rod to a high-precision linear displacement transducer. Then α is calculated from the following relationship:

$$\alpha = \frac{1}{L_0}\frac{dL}{dT} \tag{2}$$

where $L_0$is the initial length of the specimen and $dL/dT$is the temperature-dependent change in length.

The full system (Fig. 2) consists in a fused-silica tube (60 mm-OD, 55 mm-ID) around which a 1250 W ceramic band heater is installed. The heater is controlled by a PID temperature controller (*OMRON* mod. EC5N) that regulates the temperature of the heated chamber based on the inputprovided by a type-K thermocouple. This sensor is positioned at the midpoint of the tube to ensure an accurate temperature control within the measurement section. A second thermocouple is used to monitor the temperature inside the test space and is located next to the specimen, at its mid-height. This is possible by a retaining ring with set screw that allows the controlled sliding of the thermocouple. Its positioning is further helped by the a centering ceramic plate located on top of the tested sample.

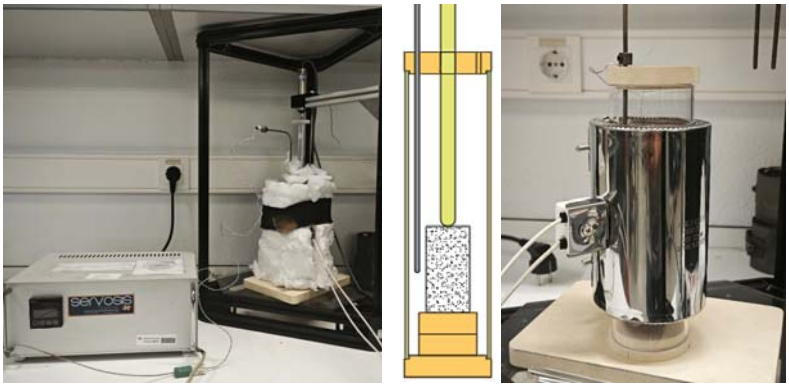


Fig. 2 General view of the push-rod dilatometer (*left*) and detail of the fused quartz tube (*center*) and with the band heater (*right*).

To attenuate external thermal oscillations (specially below 100 °C), the fused-silica tube and heater assembly are wrapped with a heat-resistant thermal-insulation blanket. Additional insulation is provided by two *cordierite* ceramic caps: One at the bottom, without openings, and a second one on top of the fused-silica tube with five perforations which allow the installation of additional temperature monitoring sensors and also provides a passage for the fused-silica push rod. The sample itself is located over a fused-silica pedestal whose height ensures that it is within the bounds of the homogeneous heating volume that is located at the mid-height of the band heater.

The push-rod is made of fused-silica and has 10 mm-diameter and 200 mm-length. The end in contact with the flat top surface of the rock specimen is machined to a hemispherical shape using a diamond grinding wheel to ensure a discrete, point-like contact. The opposite end of the push-rod is milled flat to provide a reliable reference surface for mounting a *Micro-Measurements* HS-10 linear displacement transducer (maximum travel range = 12.7 mm). Temperature measurements are acquired using a 20-bit, 8-channel USB thermocouple data logger (*Pico Technologies* mod. TC-08). When used with type-K thermocouples, this system provides a maximum resolution of 0.025 °C over the temperature range going from −250 °C to 1370 °C. Displacement measurements from the HS-10 transducer is recorded using a 24-bit, 8-channel differential signal-conditioning and acquisition unit (*Pico Technologies* mod. ADC-24).

Since thermal expansion operates over multiple elements of the experimental device (push rod, sample pedestal, test sample, etc.), in order to obtain an accurate and representative α value a number of corrections are required. Thus, to the raw thermal-expansion value (α_{raw}) it must be subtracted the sum of the contributions associated with the expansion of the heat-sensitive system elements (α_{system}). Accordingly, the corrected specimen coefficient is therefore obtained from:

$$\alpha_{sample} = \alpha_{raw} - \alpha_{system} \tag{3}$$

To determine the α_{system}, we have used - fused silica specimens as reference material (α_{sample}= α_{fused_silica}= 0.55 × 10^{-7} K^{-1} between 20 and 320 °C; White, 1973).

2.3 Thermal conductivity

Thermal conductivity governs the rate at which heat propagates through the rock mass according to Fourier's law. In this case, we have developed an enhanced steady state divided-bar apparatus based on the ASTM E1225 standard as well as the ISRM SM (Popov *et al*., 2016).

Figure 3illustrates the experimental device developed. It was designed to accommodate cylindrical rock plugs with diameters up to 54 mm and thicknesses typically ranging from 5 to 30 mm. It consists of a vertical assembly in which a disk-shaped rock specimen is placed between two identical measurement stacks composed of two high-thermal conductivity disk plates (CW614N brass, 50 mm-diameter; 10-mm-thick) and a reference disk of known thermal conductivity (fused-silica, 50 mm-diameter; 9 mm-thick). Radial bores drilled to the center of the brass plates allow the insertion of type-K thermocouples connected to a high-precision temperature acquisition system (*Pico Technologies* mod. TC-08). Heat is supplied from the lower side of the system by means of a 50 mm-diameter Inconel® 600 (UNS N06600) cylindrical platen heated by a 250 W ceramic band heater controlled through a PID controller (*Inkbird* mod. ITC-100VH). This configuration allows operating temperatures of up to ~500 °C. At the opposite end, heat is removed using an aluminium cooling reservoir connected to a recirculating cryothermostat (*J.P. Selecta Frigiterm*, model TFT-30) capable of maintaining the coolant temperature down to −30 °C, thereby establishing a controlled thermal gradient across the specimen–stack assembly. To minimize thermal contact resistance between components, the system incorporates a loading frame composed of threaded bars and a crosshead that applies a small axial seating load. The entire setup is enclosed within a sealed aluminium bell jar connected to a vacuum pump, which suppresses convective heat transfer and reduces external thermal disturbances.

Under steady-state conditions, the temperatures recorded by the thermocouples in the brass plates are used to determine the heat flux through the fused-silica reference disks and the temperature gradient across the specimen, allowing the axial thermal conductivity of the rock to be calculated according to Fourier's law:

$$q = -\lambda \frac{dT}{dx} \tag{4}$$

where q is the heat flux, λ is the thermal conductivity and dT/dx is the temperature gradient across the specimen.

$$\lambda = \frac{\lambda_c}{2(T_6 - T_5)}\left[\frac{(T_4 - T_5)}{L_1} + \left(\frac{(T_6 - T_7)}{L_3}\right)\right] \tag{5}$$

In Eq.(5), λ_c is the known thermal conductivity of the fused-silica reference disks (1.38 W/m·K), temperatures T_4 and T_5 correspond to the sensors located near the hot side, and T_6 and T_7 to those near the cold side. Likewise, L_1 and L_3 denote the axial separation distances between the corresponding pairs of temperature sensors.

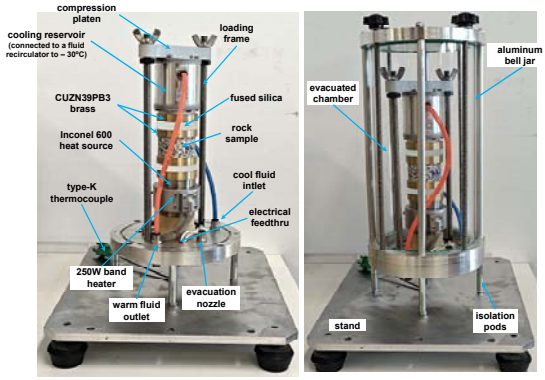


Fig. 3 Split bar thermal conductivity device with the identification of the main elements.

3 Results and discussion

Figure 4illustratesa good fit between the measured and reported heat capacity data of α-Al_2O_3(Furukawa et al., 1956), which was used for verification of the performance of the drop calorimeter. In the same figure we also present the results obtained for up to seven different rock types

which, in addition, have been fitted with the Maier-Kelley function (C_P=A+BT+CT^{-2}; Maier and Kelley, 1932). As expected, we observe that the specific heat of the rocks increases with temperature.

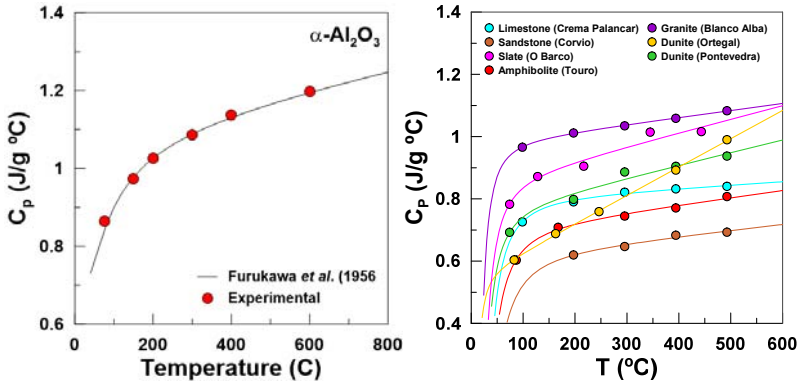


Fig. 4 *Left*: Comparison of specific heat capacity of α-Al_2O_3 measured (dots) and reported by Furukawa *et al*. (1956) (line). *Right*: $C_p$of different rocks (dots) and fitting with the Maier-Kelly function.

The limestone (*Crema Palancar*) shows C_p values between 0.73 and 0.85 J g^{-1} $ºC^{-1}$, aligning closely with the reference interval of 0.71–1.72 J g^{-1} $ºC^{-1}$ given by Schön (2015). The sandstone (*Corvio*) displays C_p values between 0.61 and 0.69 J g^{-1} $ºC^{-1}$, slightly below the wide reference range of 0.75 to3.33 J g^{-1} $ºC^{-1}$ reported by Schön (2015). This is likely due to the significant porosity of this rock (~22%) compared with other sedimentary analogues reported in the literature. In contrast, rocks with significant quartz content (such as the *O Barco* slate and the *Blanco Alba* granite) display C_p values (0.78 to 1.02 J g^{-1} $ºC^{-1}$ and 0.97 to 1.08 J g^{-1} $ºC^{-1}$, respectively) that lay towards the upper bound of their range: 0.88 to1.44 J g^{-1} $ºC^{-1}$ for slate and 0.67 to1.55 J g^{-1} $ºC^{-1}$ for granite (Schön, 2015). This behaviour is consistent with the greater heat capacity of quartz compared with other rock-forming minerals. The amphibolite rock (*Touro*) exhibits C_P values between 0.60 and 0.80 J g^{-1} $ºC^{-1}$, slightly exceeding the single reference value of 0.75 J g^{-1} $ºC^{-1}$ reported by Schön (2015). This deviation may reflect differences in amphibole mineralogy or subtle variations in bulk chemistry, both of which affect the heat capacity of mafic rocks. Finally, the two dunite samples (*Ortegal* and *Pontevedra*) show C_p values between 0.60 and 1.10 J g^{-1} $ºC^{-1}$, fully consistent with published ranges for olivine-rich ultramafic rocks, 0.55 to1.09 J g^{-1} $ºC^{-1}$ (Schön, 2015). The previous comparisons are based on the experimental temperature range (~100 to ~600 ºC) and the reported values at 25 ºC. For all studied samples, the classical Maier–Kelley formulation adequately captures the temperature dependence of heat capacity.

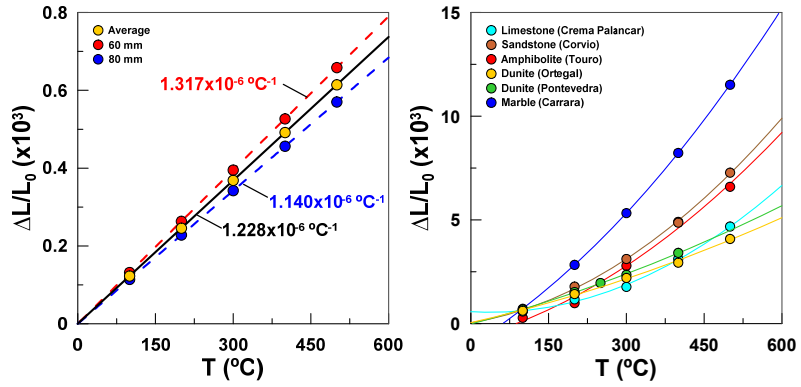


Fig. 5 *Left*: Assessment of the system correction factor for thermal expansion measurements based on two fused-silica rods of 60 and 80 mm-length and their corresponding average. *Right*: Thermal expansion of the different rocks tested.

Figure 5shows assessment of the correction factor applicable to thermal expansion determinations performed with the experimental device based on the observation of two fused-silica rods of different lengths and known α-value (5.5x10^{-7} $ºC^{-1}$). Compared with the actual rock results, we observe that the magnitude of this correction, being relevant, is comparatively small. On the right side of the same figure, the results obtained with the different rocks of interest are also displayed. In general, the data trends can be described well bya third-order polynomial equation (α(T)=A+BT+CT^2), which is considered a sufficient approach to capture the temperature-dependence of Einstein's anharmonicity at moderate temperatures (Blancas et al., 2024).The *Crema Palancar* limestone shows a measured α of 10.1×10^{-6} $ºC^{-1}$, a value close to the lower bound of the reported reference interval (10 to 30×10^{-6} $ºC^{-1}$;

Daoudi, 2025). The *Corvio* sandstone and *Touro* amphibolite exhibit measured α-values of 16.4×10^{-6} ºC^{-1} and 16.5×10^{-6} ºC^{-1}, respectively, both well within their reference ranges (11 to 20×10^{-6} ºC^{-1} (Schön, 2015) and 16 to 32 $\times10^{-6}$ ºC^{-1}(Ma, 2017) respectively. The *Blanco Alba* granite shows a thermal expansion value of 13.9×10^{-6} ºC^{-1}, in line with the reference literature (10 to 16×10^{-6} ºC^{-1}; Schön, 2015) while both dunites (*Ortegal* and *Pontevedra*) display a moderate difference likely due to mineralogical differences or variable serpentinization (with $\alpha= 9.0\times10^{-6}$ ºC^{-1} and 8.4×10^{-6} ºC^{-1} for the *Pontevedra* and *Ortegal* specimens, respectively). In any case, both values fall in the lower bound of the reported range from 8 to 12×10^{-6} ºC^{-1} (Suzuki, 1975). Finally, the *Carrara* marble shows the highest thermal expansion ($\alpha = 27.0\times10^{-6}$ ºC^{-1}) among the tested rocks although closely matching the reference value of ~29×10^{-6} ºC^{-1} (Daoudi, 2025).

The thermal conductivity results obtained with the enhanced divided-bar equipment are presented in Fig.6.On its left-hand side, we present a thermal map of the heating chamber at 300 ºC illustrating the homogeneous temperature distribution in the area of insertion of the specimen. The reported temperatures correspond to those at the mid-height of the combined rock-reference stacks, which is also the location of the mid-height of the tested specimens. It is worth noting that, while for some rocks λ may be represented by a single, constant slope (*e.g.* dunites) for the rest a better fit may be achieved using the Zoth & Haenel (1988) function ($\lambda(T) = A + B(350 + T)$, with T in ºC). For the tested rocks, λ becomes smaller, an aspect already highlighted by other authors (Lee & Deming, 1988).

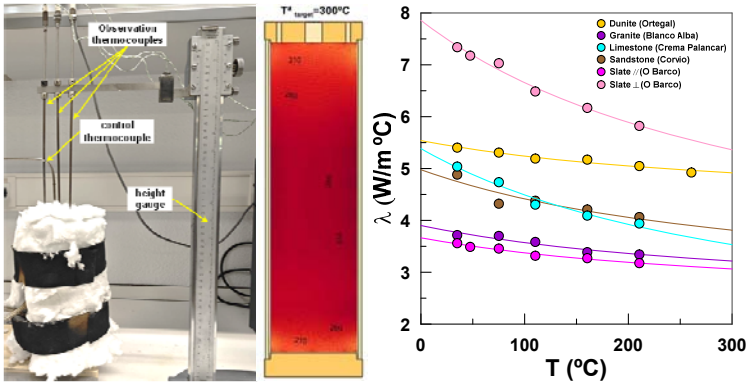


Fig.6 *Left*: Experimental arrangement to obtain temperature maps of the heating chamber; *Center*: Temperature distribution in the heating chamber at 300 ºC; *Right*: Thermal conductivity (λ) results of the studied rocks.

Comparing only 25 ºC data, we see that, for the *Crema Palancar* limestone, thermal conductivity is 13.87 $Wm^{-1}{}^{o}C^{-1}$ while for the *Corvio* sandstone this is 4.93 $Wm^{-1}{}^{o}C^{-1}$, both close to the reference values of 16.2 $Wm^{-1}{}^{o}C^{-1}$and 2.4 to 4.76 $Wm^{-1}{}^{o}C^{-1}$, respectively, reported byRao (2022). The *O Barco* slate reveals a strong thermal anisotropy, with λ- values higher when the specimens are cut parallel to foliation than when perpendicular to it. This behavior has been already documented in the literature (*e.g.* Xiel, 2025). The *Blanco Alba* granite has a thermal conductivity of 3.74 W m^{-1} °C^{-1}, a value consistent with data available in the literature (1.25 to 4.45 W m^{-1} ºC^{-1}; Schön, 2015).Finally, the *Ortegal* dunite exhibits an intermediate conductivity (5.38 W m^{-1} °C^{-1}), also in good agreement with the reference data of 4 to 11.5 W m^{-1} °C^{-1} reported by Zeb (2010). Such value would correspond to an olivine-rich, ultramafic rocks with little serpentinization, as serpentine phases tend to reduce thermal conductivity.

4 Conclusions

The series of experimental devices presented are useful to assess thermal properties of rocks using plug-size specimens at above ambient temperature conditions, expanding and enhancing the limits of the currently available ISRM SM. The results highlight the relevance of mineralogy, porosity, anisotropy, alteration degree, and temperature dependence, demonstrating that these properties cannot be treated as constants. Their determination is therefore essential for engineering applications, as neglecting thermal effects may lead to inaccurate designs, unexpected deformations, or reduced safety, so these tests should be considered mandatory whenever thermal loads are involved.

Acknowledgements

This work has been funded by Repsol S.A. (Near-Wellbore Project). A.M.I. acknowledges support from the European Union's Horizon Europe Research and Innovation programme under the *Marie Skłodowska-Curie* grant agreement No. 101106038. Y.L. gratefully acknowledges the financial support from the *China Scholarship Council* (No. 202206560006).

References

ASTM International (2016) ASTM D4611-16: Standard test method for specific heat of rock and soil. ASTM International, West Conshohocken, PA.

ASTM International (2022) ASTM E228-22: Standard test method for linear thermal expansion of solid materials with a push-rod dilatometer. ASTM International, West Conshohocken, PA

ASTM International (2020) ASTM E1225-20: Standard Test Method for Thermal Conductivity of Solids Using the Guarded-Comparative-Longitudinal Heat Flow Technique. ASTM International, West Conshohocken, PA

Blancas EJ, Lobato Á, Izquierdo-Ruiz F, Márquez AM, Recio JM, Nath P, Plata JJ & Otero-de-la-Roza A (2024). Thermodynamics of solids including anharmonicity through quasiparticle theory. npj Computational Materials 10, 267

Daoudi A, Tadie V, Eslami J, Beaucour AL, Pani C, &Noumowé A (2025) High-temperature performance of limestone-based masonry: Investigations at the material and assembly scales. *Case Studies in Construction Materials* 23, e05361.

Furukawa GT, Douglas TB, McCoske RE & Ginnings DC (1956) Thermal properties of aluminum oxide from 0° to 1,200° K. *Journal of Research of the National Bureau of Standards* 57, 67-82

ISRM (1979) Suggested methods for determining the uniaxial compressive strength and deformability of rock materials. *International Journal of Rock Mechanics and Mining Sciences* 16, 135–140

Labus M, Labus K (2018) Thermal conductivity and diffusivity of fine-grained sedimentary rocks. *Journal of Thermal Analysis and Calorimetry* 132, 1669–1676

Lee Y & Deming D (1998) Evaluation of thermal conductivity temperature corrections applied in terrestrial heat flow studies. *Journal of Geophysical Research* 103, 2447-2454

Ma Z, Tang F, Qi F, & Lian Y (2017) Experimental study on thermal expansion coefficient changing rule of sandstone under high temperature. *Journal of Mining Science and Engineering* 1, 019.

Maier GG, Kelley HK (1932) An equation for the presentation of the high-temperature heat content data. *Journal of the American Chemical Society* 54, 3243–3246

Popov Y, Beardsmore G, Clauser C, &Roy S (2016) ISRM Suggested Methods for determining thermal propertiesof rocks from laboratory tests at atmospheric pressure. *Rock Mechanics and Rock Engineering*49, 4179–4207

Rao SE, Ray L, Khan T, & Ravi G (2022) Thermal conductivity, density and porosity of sedimentary and metamorphic rocks from the Lower and Higher Himalaya, Western Himalaya, India. *Geophysical Journal International* 231, 459-473.

Righetti MC, Salvetti G,& Tombari, E (1998) Heat capacity of glycerol from 298 to 383 K. *Thermochimica Acta* 316, 193-195

Schön JH (2015) Physical Properties of Rocks: Fundamentals and Principles of Petrophysics. 2nd Ed. Elsevier, Amsterdam

Suzuki I (1975) Thermal expansion of periclase and olivine, and their anharmonic properties. *Journal of the Physical Society of Japan - Earth Sciences*, 23, 145-159.

White GK (1973) Thermal expansion of reference materials: copper, silica and silicon. *Journal of Applied Physics D Applied Physics* 6, 2070–2078

Xie L, Yu C, Zhang Y, He B, Wang R, & Liu J (2025) Multiscale and quantitative study of thermal conductivity in shale using TDTR measurements and homogenization techniques. *Applied Clay Science*, 267, 107719.

Zeb A, Firdous T, & Maqsood A (2010) Thermophysical properties of dunite rocks as a function of temperature along with the prediction of effective thermal conductivity. *Natural Science* 2, 626-630.

Zoth G & Haenel R (1988) Thermal Conductivity, in *Handbook of Terrestrial Heat-Flow Density Determination*, R. Haenel, L. Rybach& L. Stegena Eds. p. 449-453, Kluwer Acad., Norwell, Mass

Zhu C, Chen C, Yang Y & Qiu N (2022) Experimental study into the factors influencing rock thermal conductivity. *Petroleum Science Bulletin*7, 321-333